Available online at www.sciencedirect.com
ScienceDirect
Journal of Sound and Vibration 297 (2006) 595–615
JOURNAL OF SOUND AND VIBRATION
www.elsevier.com/locate/jsvi

A finite element transient response analysis method of a rotor-bearing system to base shock excitations using the state-space Newmark scheme and comparisons with experiments

An Sung Lee[a,*], Byung Ok Kim[a], Yeong-Chun Kim[b]

[a]*Rotor Dynamics Team, Korea Institute of Machinery and Materials, Yoosung, P.O. Box 101, Daejeon, 305–600, Republic of Korea*
[b]*R&D Center, Doosan Heavy Industries Co., 555 Guygok-dong, Changwon, 641–792, Gyeongnam, Republic of Korea*

Received 18 April 2005; received in revised form 1 February 2006; accepted 10 April 2006
Available online 13 July 2006

Abstract

Turbomachinery such as turbines, pumps and compressors, which are installed in transportation systems, including aircraft, ships and space vehicles, etc., often perform their critical missions and are exposed to potential dangerous impact environments such as base-transferred shock forces. In this study a transient response analysis technique of a rotor system is proposed. The study involves applying the generalized finite element modeling method of a rotor-bearing system considering a base-transferred shock force along with the state-space Newmark method of a direct time integration scheme based on the average velocity concept. Experiments are performed to a test rig of a mock-up rotor-bearing system with a series of half-sine shock waves imposed by an electromagnetic shaker, and quantitative error analyses between analytical and experimental results are carried out. The results show that the transient responses of the rotor are sensitive to the duration times of the shocks. In particular, in cases where the frequencies, $1/(2 \times \text{duration time})$, of the shock waves are close to the critical speed of the rotor-bearing system, resonances may occur and the transient responses of the rotor are consequently amplified. Overall, the analytical results agree quite well with the experimental data.
Published by Elsevier Ltd.

1. Introduction

Turbomachinery such as turbines, pumps and compressors, which are installed in transportation systems, including aircrafts, ships and space vehicles, etc., often experience various sudden shock forces through their life cycles, depending on the operating conditions and external environment. These shock forces may be transferred through bases or foundations directly to core rotor-bearing systems of turbomachinery, and can induce severe damages due to direct impact collisions between the rotors and bearings, seals and other stators or generate dangerous high vibrations in the rotors due to their rubbing contacts. Therefore, in cases of turbomachinery which are exposed to potential dangerous impact environment and still perform their critical missions, it is necessary to accurately predict transient responses of their rotor systems under base-transferred shock forces and estimate their safety in the early design stages.

*Corresponding author. Tel.: +42 868 7356; fax: +42 868 7440.
E-mail addresses: aslee@kimm.re.kr (A.S. Lee), kbo2612@kimm.re.kr (B.O. Kim).

0022-460X/$ - see front matter Published by Elsevier Ltd.
doi:10.1016/j.jsv.2006.04.028

Transient response analyses of rotor-bearing systems to base-transferred shock forces might be classified into system modeling methods and types of excitations. Hori and Kato [1] investigated the stability of a rotor system supported by fluid film bearings when acted by seismic loads, using a Jeffcott rotor model. Tessarzik et al. [2] analyzed transient responses of a simple turbomachinery model, considering relative coordinate systems, to random excitations in the axial direction imposed at its base, and Soni and Srinivasan [3] investigated the responses of a rigid rotor model to seismic loads. Singh et al. [4], Suarez et al. [5], and Gaganis et al. [6] proposed finite element(FE) rotor models by taking their base motions into consideration and analyzed transient responses to seismic excitations. It is noteworthy that Suarez et al. [5] proposed the most generalized rotor-bearing system model with base excitations by introducing parametric and nonlinear effects, induced by the rotational motions of the base, into their model.

As direct time-integration methods for obtaining a transient response of a dynamic system, there is an explicit method such as the Runge–Kutta method and an implicit method such as the Newmark method. However, generally speaking, since in the explicit method a time step, Δt, acts as a quite restrictive condition for numerical stability, for a dynamic system with large degrees of freedom, the implicit method which has a numerical stability for any Δt [7] is frequently utilized. Among the implicit methods, the Newmark method based on the average acceleration is most widely used. This method has a guaranteed numerical stability and second-order accuracy [8]. For a rotor-bearing system in which its bearing stiffness or damping is generally asymmetric and unproportional to its system inertia or stiffness, an eigenvalue analysis is often performed by transforming the system equation into a first-order differential equation by introducing the state-space vector. On the other hand, the conventional Newmark method based on the average acceleration cannot be directly applied to solve a transient response of the state-space first-order differential equation. To overcome this, Kim and Lee [9] proposed the state-space Newmark method, which is based on the average velocity concept.

Most of the above previous studies concentrated on constructing reliable analytical models depending on the types of base excitations, and only a few investigations have been carried out to verify the analytical models through experiments or to estimate the quantitative errors of dynamic transient responses. In this study a transient response analysis technique of a rotor system is proposed. The methods involves applying the generalized FE modeling method of a rotor-bearing system considering the base-transferred shock force along with the state-space Newmark method of a direct time integration scheme based on the average velocity concept. Experiments are performed to a test rig of mock-up rotor-bearing system with a series of half-sine waves imposed by an electromagnetic shaker, and quantitative error analyses between analytical and experimental results are also carried out.

2. Equation of motion

2.1. Energy equation

Fig. 1 shows a rotor-bearing system mounted on its rigid base, and XYZ is the inertial reference frame and xyz the local reference coordinate system attached to the base. At a certain point, P, along the centerline of the rotor shaft, u_x, u_y, θ_x and θ_y represent translational and rotational displacements in the x and y directions. The

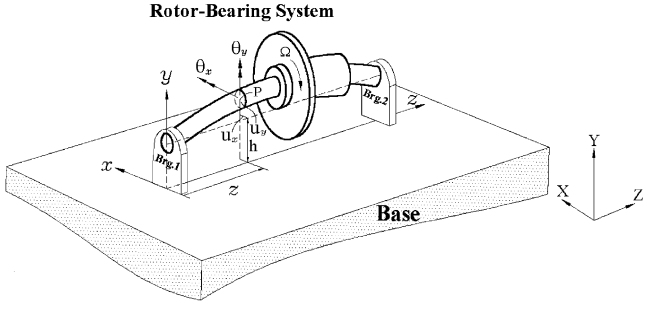

Fig. 1. Rotor-bearing system on the rigid base and its coordinate systems.

rotor rotates at a constant angular velocity of Ω with respect to the z-axis and any displacement in the z direction is neglected. Further, u_{bX}, u_{bY}, u_{bZ}, θ_{bX}, θ_{bY} and θ_{bZ} represent translational and rotational displacements of the base with respect to XYZ, respectively.

Considering a position vector, $\{r_b\}$, of xyz from XYZ and a position vector, $\{r\}$, of P from xyz, a velocity vector of P is expressed by

$$\{\dot{r}_P\} = \{\dot{r}_b\} + \{\dot{r}\} + [\omega_b]\{r\}, \tag{1}$$

where

$$\{r\} = \lfloor u_x \quad u_y + h \quad z \rfloor^{\mathrm{T}}, \quad \{\dot{r}_b\} = \lfloor \dot{u}_{bX} \quad \dot{u}_{bY} \quad \dot{u}_{bZ} \rfloor^{\mathrm{T}},$$

$$\{\dot{r}\} = \lfloor \dot{u}_x \quad \dot{u}_y \quad 0 \rfloor^{\mathrm{T}}, \quad [\omega_b] = \begin{bmatrix} 0 & -\dot{\theta}_{bZ} & \dot{\theta}_{bY} \\ \dot{\theta}_{bZ} & 0 & -\dot{\theta}_{bX} \\ -\dot{\theta}_{bY} & \dot{\theta}_{bX} & 0 \end{bmatrix}.$$

Considering the translational and rotational motion of a disk element, representing a lumped mass at P, its kinetic energy is expressed by

$$T_d = \tfrac{1}{2} m_d \{\dot{r}_P\}^{\mathrm{T}} \{\dot{r}_P\} + \tfrac{1}{2} \{\omega\}^{\mathrm{T}} [I_d] \{\omega\}, \tag{2}$$

where m_d is a mass of the disk element, and $\mathrm{diag}[I_d] = \{I_d^t \quad I_d^t \quad I_d^p\}$ and I_d^t and I_d^p are the transverse and polar moments of inertia of the disk element, repectively. An angular velocity vector, $\{\omega\}$, of the shaft can be expressed by the following, utilizing the Euler angles α, β and γ:

$$\{\omega\} = \begin{bmatrix} \cos\beta\cos\gamma & \sin\gamma & 0 \\ -\cos\beta\sin\gamma & \cos\gamma & 0 \\ \sin\beta & 0 & 1 \end{bmatrix} \begin{Bmatrix} \dot{\alpha} \\ \dot{\beta} \\ \dot{\gamma} \end{Bmatrix}, \tag{3}$$

where $\alpha = \theta_x + \theta_{bX}$, $\beta = \theta_y + \theta_{bY}$ and $\gamma = \Omega t$. Substituting Eqs. (1) and (3) into Eq. (2), the kinetic energy of the disk element is

$$\begin{aligned} T_d = \frac{m_d}{2} (&\{\dot{r}_b\}^{\mathrm{T}} \{\dot{r}_b\} + \{\dot{r}\}^{\mathrm{T}} \{\dot{r}\} - \{r\}^{\mathrm{T}} [\omega_b]^2 \{r\} + 2\{\dot{r}\}^{\mathrm{T}} [\omega_b] \{r\} + 2\{\dot{r}_b\}^{\mathrm{T}} \{\dot{r}\} \\ &+ 2\{\dot{r}_b\}^{\mathrm{T}} [\omega_b] \{r\}) + \tfrac{1}{2} (I_d^t \{\dot{\Theta}\}^{\mathrm{T}} \{\dot{\Theta}\} + 2\Omega I_d^p \{\dot{\Theta}\}^{\mathrm{T}} \{e_1\} \{e_2\}^{\mathrm{T}} \{\Theta\} + \Omega^2 I_d^p), \end{aligned} \tag{4}$$

where $\{\Theta\} = \lfloor \theta_x + \theta_{bX} \quad \theta_y + \theta_{bY} \rfloor^{\mathrm{T}}$, $\{e_1\} = \lfloor 1 \quad 0 \rfloor^{\mathrm{T}}$ and $\{e_2\} = \lfloor 0 \quad 1 \rfloor^{\mathrm{T}}$ and $\{e_2\} = \lfloor 0 \quad 1 \rfloor^{\mathrm{T}}$. Referring to the shaft element as shown in Fig. 2 and considering its translational and rotational motions, its kinetic energy is expressed by

$$T_s = \int_0^l \frac{1}{2} \rho A \{\dot{r}_P\}^{\mathrm{T}} \{\dot{r}_P\} \, \mathrm{d}\xi + \int_0^l \frac{1}{2} \rho \{\omega\}^{\mathrm{T}} [I_s] \{\omega\} \, \mathrm{d}\xi, \tag{5}$$

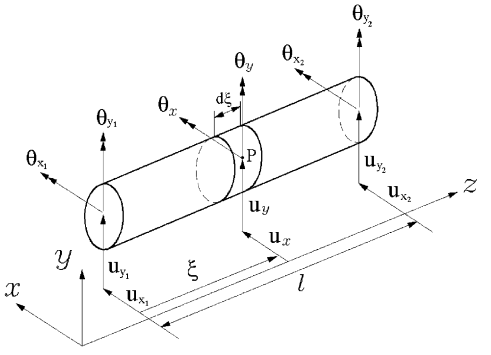

Fig. 2. Shaft element and its coordinate system.

where ρA is the mass per a unit length of the shaft element, and $\mathrm{diag}[I_s] = \{I_s^t I_s^t I_s^p\}$ and I_s^t and I_s^p are the transverse and polar area moments of inertia of the shaft element, respectively. Substituting Eqs. (1) and (3) into Eq. (5), the kinetic energy of the shaft element is

$$T_s = \int_0^l \frac{1}{2}\rho A(\{\dot{r}_b\}^{\mathrm{T}}\{\dot{r}_b\} + \{\dot{r}\}^{\mathrm{T}}\{\dot{r}\} - \{r\}^{\mathrm{T}}[\omega_b]^2\{r\} + 2\{\dot{r}\}^{\mathrm{T}}[\omega_b]\{r\} + 2\{\dot{r}_b\}^{\mathrm{T}}\{\dot{r}\} + 2\{\dot{r}_b\}^{\mathrm{T}}[\omega_b]\{r\})\,\mathrm{d}\xi + \int_0^l \frac{1}{2}\rho(I_s^t\{\dot{\Theta}\}^{\mathrm{T}}\{\dot{\Theta}\} + 2\Omega I_s^p\{\dot{\Theta}\}^{\mathrm{T}}\{e_1\}\{e_2\}^{\mathrm{T}}\{\Theta\} + \Omega^2 I_s^p)\,\mathrm{d}\xi. \tag{6}$$

Considering the bending and shear deformations of the shaft element, its strain energy is expressed by

$$V_s = \int_0^l \frac{1}{2}[EI_s^t\{\theta'\}^{\mathrm{T}}\{\theta'\} + \kappa GA\{\theta_s\}^{\mathrm{T}}\{\theta_s\}]\,\mathrm{d}\xi, \tag{7}$$

where $\{\theta\} = \lfloor \theta_x \quad \theta_y \rfloor^{\mathrm{T}}$, $\{\theta_s\} = \left\lfloor u_y' + \theta_x \quad u_x' - \theta_y \right\rfloor^{\mathrm{T}}$, and E is the Young's modulus, G the shear modulus and κ the shear coefficient of the shaft element, and $'$ represents $\partial/\partial\xi$.

2.2. FE equation of motion

Applying the Lagrange's equation to the kinetic energy of the disk element given by Eq. (4), the equation of motion of the disk element may be expressed by the following:

$$[M_d]\{\ddot{q}_d\} + [C_d]\{\dot{q}_d\} + [K_d]\{q_d\} = \{f_{d1}(t)\} + \{f_{d2}(t)\} + \{f_{d3}(t)\}, \tag{8}$$

where $\{q_d\} = \lfloor u_x \quad u_y \quad \theta_x \quad \theta_y \rfloor^{\mathrm{T}}$, and the system matrices and forcing vectors are given in the Appendix A. Different from the conventional equation of motion of a disk element [10], Eq. (8) contains in $[C_d]$ the parametric term due to the angular velocity of the base in addition to the gyroscopic effect term and has the newly generated $[K_d]$, comprised of the parametric terms due to the products of the angular velocities and the angular acceleration of the base. The generalized excitation force also consists of $\{f_{d1}(t)\}$ due to the translational acceleration of the base, the nonlinear $\{f_{d2}(t)\}$ generated by the products of the translational and angular velocities of the base and $\{f_{d3}(t)\}$ due to the angular velocity and acceleration of the base.

Referring to Figs. 1 and 2, at point P in the shaft element $\{r\}$, $\{\theta\}$ and $\{\theta_s\}$ are expressed by

$$\{r\} = \begin{Bmatrix} u_x \\ u_y + h \\ z \end{Bmatrix} = \begin{Bmatrix} u_x \\ u_y \\ 0 \end{Bmatrix} + \begin{Bmatrix} 0 \\ h \\ z \end{Bmatrix} = \{u\} + \{e\} = [N_t]\{q_s\} + \{e\}, \tag{9}$$

$$\{\theta\} = \begin{Bmatrix} \theta_x \\ \theta_y \end{Bmatrix} = [N_r]\{q_s\}, \tag{10}$$

$$\{\theta_s\} = \begin{Bmatrix} u_y' + \theta_x \\ u_x' - \theta_y \end{Bmatrix} = [N_s]\{q_s\}, \tag{11}$$

where $\{q_s\} = \lfloor u_{x_1} \quad u_{y_1} \quad \theta_{x_1} \quad \theta_{y_1} \quad u_{x_2} \quad u_{y_2} \quad \theta_{x_2} \quad \theta_{y_2} \rfloor^{\mathrm{T}}$ and $\{e\} = \lfloor 0 \quad h \quad z \rfloor^{\mathrm{T}}$ and $[N_t]$, $[N_r]$ and $[N_s]$ are the shape function matrices of the translational, rotational, shear rotary displacements of the shaft element [10]. Substituting Eqs. (9)–(11) into the kinetic and strain energies of the shaft element given by Eqs. (6) and (7), and applying the Lagrange's equation to them, the FE equation of motion of the shaft element may be expressed by the following:

$$\begin{aligned}&([M_s^t] + [M_s^r])\{\ddot{q}_s\} + (\Omega[C_s^g] + \dot{\theta}_{bZ}[C_s^p])\{\dot{q}_s\} + ([K_s^e] + [K_s^c] + \ddot{\theta}_{bZ}[K_s^a])\{q_s\} \\ &= \{f_{s1}(t)\} + \{f_{s2}(t) + \{f_{s3}(t)\}\end{aligned} \tag{12}$$

where the system matrices and forcing vectors are given in the Appendix B. Similarly, different from the conventional equation of motion of the shaft element [10], Eq. (12) contains in the generalized damping matrix

the parametric term $\dot{\theta}_{bZ}[C_s^p]$ due to the angular velocity of the base in addition to the gyroscopic effect term $\Omega[C_s^g]$, and in the generalized stiffness matrix the parametric term $[K_s^c]$ due to the products of the angular velocities and the angular acceleration of the base and the parametric term $\ddot{\theta}_{bZ}[K_s^a]$ due to the angular acceleration of the base in addition to $[K_s^e]$, which is due to bending and shear deformations. The generalized excitation force also consists of $\{f_{s1}(t)\}$ due to the translational acceleration of the base, the nonlinear $\{f_{s2}(t)\}$ generated by the products of the translational and angular velocities of the base and $\{f_{s3}(t)\}$ due to the angular velocity and acceleration of the base.

Further considering the equations of bearing elements and external forces such as unbalance forces, an assembled-resultant equation of motion of the entire rotor-bearing system can be expressed by

$$[M]\{\ddot{q}\} + [C]\{\dot{q}\} + [K]\{q\} = \{f(t)\}. \tag{13}$$

Finally, introducing the state-space vector, Eq. (13) can be transformed into the first-order differential equation as given by

$$\{\dot{r}\} = [A]\{r\} + \{F\}, \tag{14}$$

where

$$\{r\} = \lfloor \{\dot{q}\} \quad \{q\} \rfloor^{\mathrm{T}}, \quad [A] = \begin{bmatrix} -[M]^{-1}[C] & -[M]^{-1}[K] \\ [I] & [0] \end{bmatrix},$$

$$\{F\} = \begin{Bmatrix} [M]^{-1}\{f(t)\} \\ \{0\} \end{Bmatrix}.$$

3. Transient response analysis

3.1. State-space Newmark method

As shown in Fig. 3 the state-space Newmark method assumes an average velocity over the time interval, Δt. Defining time $\tau(0 \leqslant \tau \leqslant \Delta t)$ within Δt, the average velocity between the time step t_n and t_{n+1} is

$$\{\dot{r}(\tau)\} = \tfrac{1}{2}[\{\dot{r}\}_{n+1} + \{\dot{r}\}_n]. \tag{15}$$

Integrating Eq. (15) with an initial condition, $\{\tau(0)\} = \{r\}_n$, the displacement at time τ is

$$\{r(\tau)\} = \{r\}_n + \frac{\tau}{2}[\{\dot{r}\}_{n+1} + \{\dot{r}\}_n]. \tag{16}$$

From Eq. (16), the displacement at $\tau = \Delta t$, in other words, the time step t_{n+1}, is

$$\{r\}_{n+1} = \{r\}_n + \frac{\Delta t}{2}[\{\dot{r}\}_{n+1} + \{\dot{r}\}_n]. \tag{17}$$

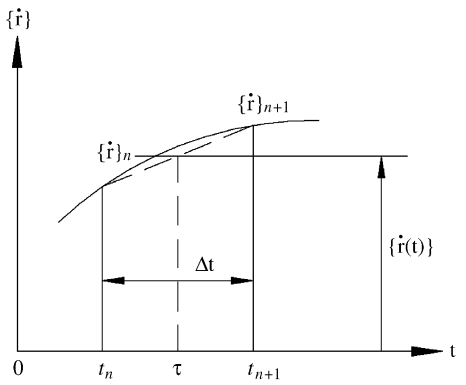

Fig. 3. Average velocity in the state-space Newmark method.

Then, the velocity at $t_{n+1}$is

$$\{\dot{r}\}_{n+1} = \frac{2}{\Delta t}[\{r\}_{n+1} - \{r\}_n] - \{\dot{r}\}_n. \tag{18}$$

Finally, considering Eq. (14) at t_{n+1}, and substituting Eq. (18) into it and manipulating,

$$\{r\}_{n+1} = ([I] - \frac{\Delta t}{2}[A])^{-1}(\{r\}_n + \frac{\Delta t}{2}\{\dot{r}\}_{n+1} + \frac{\Delta t}{2}\{F\}_{n+1}). \tag{19}$$

Upon calculating Eq. (19) with the state values at t_n the state values or displacement and velocity at t_{n+1} are obtained. Thus, the introduced state-space Newmark method yields a much simpler and more straightforward formulation than the conventional Newmark method, which is based on the average acceleration and thereby its coding is more readily carried out.

3.2. Error estimation

In order to estimate the quantitative error between analytical and experimental time responses, a magnitude error factor, ε_m, phase error factor, ε_p, and comprehensive error factor, ε_c, are explored from an analytical response $\mathbf{t}_1$ and an experimental response $\mathbf{t}_2$ A response $\mathbf{t}_2$ with its data length number of N can be expressed by the product of its magnitude m and unit vector $\mathbf{l}$:

$$\mathbf{t} = m\mathbf{l}, \tag{20}$$

where $m = \sqrt{\sum_{i=1}^{N} t(i)^2}$and $\mathbf{l} = \mathbf{t}/m$. Utilizing the phase correlation, $p_a = \mathbf{l}_1 \cdot \mathbf{l}_2$, between the two responses, ε_p is defined by the following:

$$\varepsilon_p = \frac{\cos^{-1}(p_a)}{\pi}, \quad 0 \leqslant \varepsilon_p \leqslant 1 \begin{cases} \varepsilon_p = 0 \rightarrow \text{no phase error}, \\ \varepsilon_p = 1 \rightarrow \text{out of phase}, \end{cases} \tag{21}$$

where $p_a = C/\sqrt{AB}$, $A = \sum_{i=1}^{N} t_1(i)^2$, $B = \sum_{i=1}^{N} t_2(i)^2$ and $C = \sum_{i=1}^{N} t_1(i)t_2(i)$. Utilizing the relative magnitude error, $m_a = (A - B)/\sqrt{AB}$, ε_m is defined by the following [11]:

$$\varepsilon_m = \text{sign}(m_a)\log_{10}(1 + |m_a|), \tag{22}$$

where if $\varepsilon_m = 0$ there is no magnitude error, and if $\varepsilon_m > 0$, the magnitude error may increase but it converges to a certain constant value and thereby ε_m does not diverge. Finally, from ε_m and ε_p, ε_c is defined by

$$\varepsilon_c = \sqrt{x(\varepsilon_m^2 + \varepsilon_p^2)}, \tag{23}$$

where x is a scale factor with a recommended value of $\pi/4$. On the other hand, if the absolute values of ε_m, ε_p and ε_c are all less than 0.2, the two responses are evaluated as being in good agreement with each other [11].

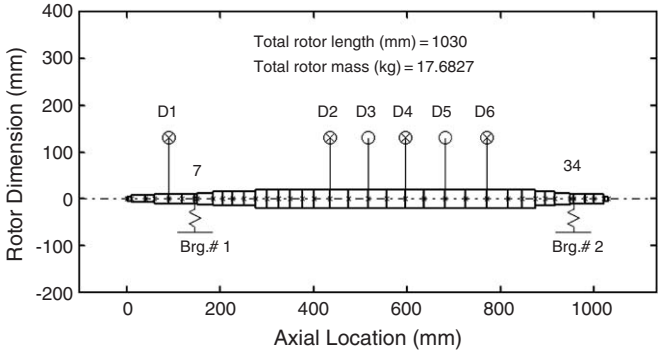

Fig. 4. Equivalent FE rotor-bearing system model.

4. Results and discussions

4.1. Numerical analysis

Fig. 4 shows an equivalent FE model of the rotor-bearing system used in the base-transferred shock transient analysis, and its detailed modeling data are given in Table 1. Its critical speeds are 3044 and 8092 rev/min. Figs. 5 and 6 show the shock excitations applied to the base of the rotor-bearing system and the transient responses of the rotor rotating at 6000 rev/min as predicted at bearing 1 and 2 positions. The shock excitation

Table 1
Detailed FE modeling data for the rotor-bearing system

Shaft element[a]

N	*L*	*D*	*N*	*L*	*D*	*N*	*L*	*D*	*N*	*L*	*D*	*N*	*L*	*D*	*N*	*L*	*D*
1	10	10	8	34	24	15	25	40	22	40	40	29	30	40	36	20	20
2	30	15	9	20	30	16	25	40	23	40	40	30	20	30	37	10	10
3	20	15	10	20	30	17	25	40	24	45	40	31	20	30			
4	28.5	20	11	25	30	18	35	40	25	45	40	32	34	24			
5	28.5	20	12	25	30	19	40	40	26	45	40	33	6	20			
6	28	20	13	25	40	20	40	40	27	45	40	34	25	20			
7	6	20	14	25	40	21	40	40	28	30	40	35	20	20			

Disk element

Disk no.	Mass (kg)	I_t (kg m^2)	I_p (kg m^2)	Unbalance (g mm)	Disk no.	Mass (kg)	I_t (kg m^2)	I_p (kg m^2)	Unbalance (g mm)
D1	0.736	3.3^E-4	2.67^E-4	$40\angle 0^\circ$	D4	1.883	2.24^E-3	4.35^E-3	$40\angle 0^\circ$
D2	1.034	7.8^E-4	1.5^E-3	$40\angle 0^\circ$	D5	2.824	3.47^E-3	6.53^E-3	—
D3	1.034	7.8^E-4	1.5^E-3	—	D6	2.824	3.47^E-3	6.53^E-3	$40\angle 0^\circ$

Bearing stiffness and damping ($K_{xy} = K_{yx} = C_{xy} = C_{yx} = 0$)

Brg. no.	K_{xx} (N/m)	K_{yy} (N/m)	C_{xx} (N s/m), $\xi = 0.01$	C_{yy} (N s/m), $\xi = 0.01$
1, 2	1.75E6	1.75E6	5.57E1	5.57E1

[a] *N*, element no.; *L*, length (mm); *D*, diameter (mm). $E = 2.0 \times 10^{11}$ N/m^2; $\rho = 7833.48$ kg/m^3.

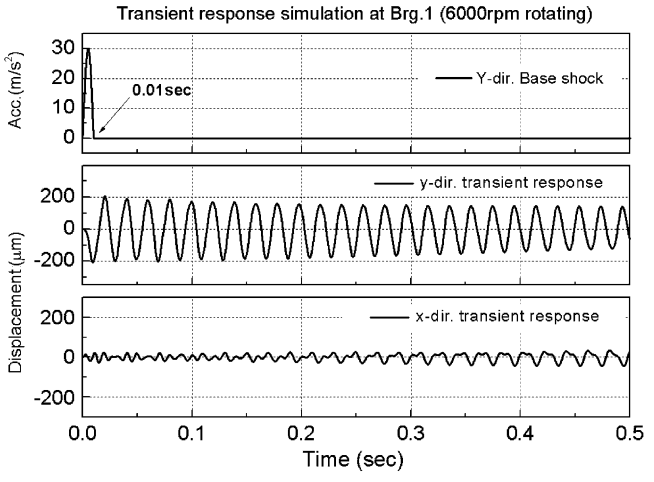

Fig. 5. Shock excitation and *y* and *x* direction rotor responses predicted at bearing 1.

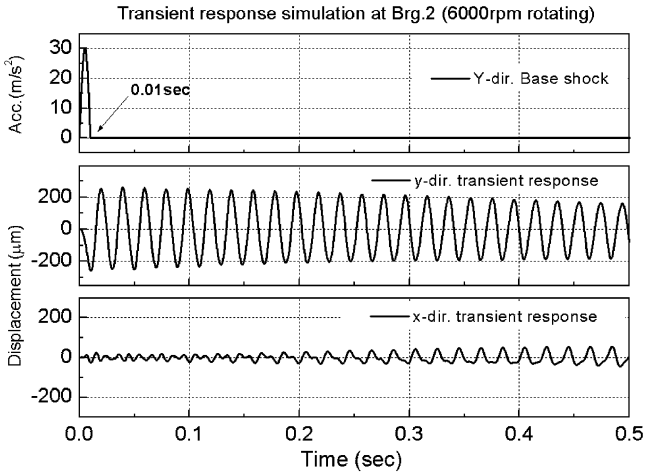

Fig. 6. Shock excitation and y and x direction rotor responses predicted at bearing 2.

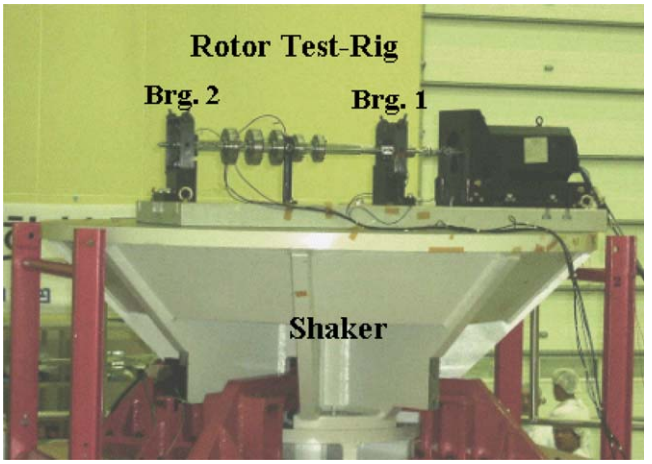

Fig. 7. Set-up of the rotor test-rig and electro-magnetic shaker.

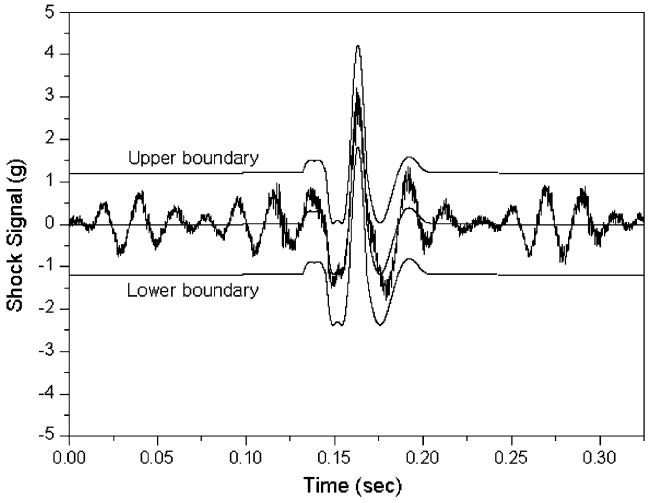

Fig. 8. A typical half-sine wave shock signal with a duration time of 10 ms generated by the electro-magnetic shaker.

was an ideal half-sine wave with a magnitude of 3g and a duration time of 10 ms, and was applied in the y direction. The maximum y direction responses of the rotor at bearings 1 and 2 were predicted to be 398.8 and 520.9 μm (Pk-to-Pk), respectively. Even though the shock was applied only in the y direction and the coupling effects of the bearings were neglected, the x direction responses of the rotor were generated due to the gyroscopic coupling effect and increased with time.

4.2. Set-up of shock experiment

A rotor test-rig, which simulates the equivalent FE rotor-bearing system shown in Fig. 4, was constructed. Fig. 7 shows a set-up of the shock experiment in which the rotor test-rig was installed on the electro-magnetic shaker, and the rotor was excited only in the vertical y direction. The test rotor was supported by two ball bearings and each bearing was installed on its pedestal through four coil springs. The resulting effective

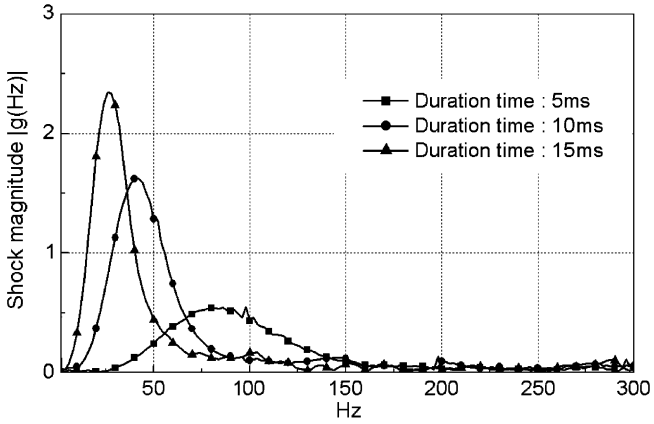

Fig. 9. Spectra of experimental half-sine wave shock excitations.

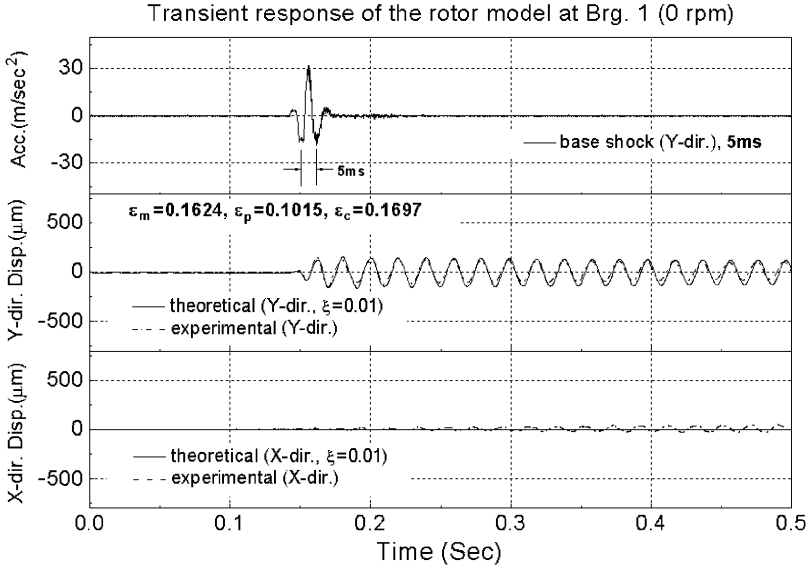

Fig. 10. Experimental shock wave with a duration time of 5 ms and analytical and experimental rotor responses at bearing 1 for 0 rev/min.

bearing stiffness was then controlled by these springs. Modal tests revealed that the first and second resonant speeds of the test rotor system were 3060 and 8076 rev/min, and thereby its natural characteristics were in good agreement with those of the analytical model in Fig. 4. Fig. 8 shows a typical example of the half-sine wave shock signal with a duration time of 10 ms generated by the electro-magnetic shaker. Fig. 9 shows spectra of the half-sine shock signals generated by the shaker with maximum accelerations of about $3g$ and duration times of 5, 10 and 15 ms.

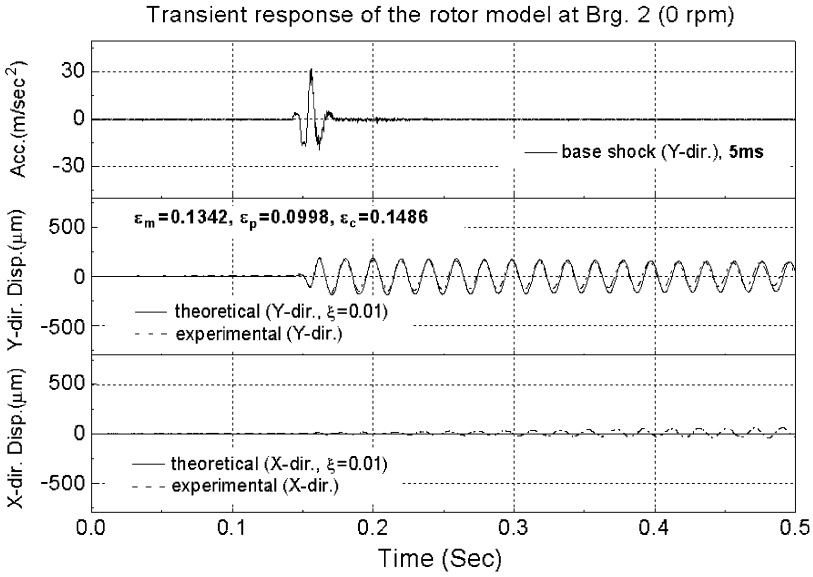

Fig. 11. Experimental shock wave with a duration time of 5 ms and analytical and experimental rotor responses at bearing 2 for 0 rev/min.

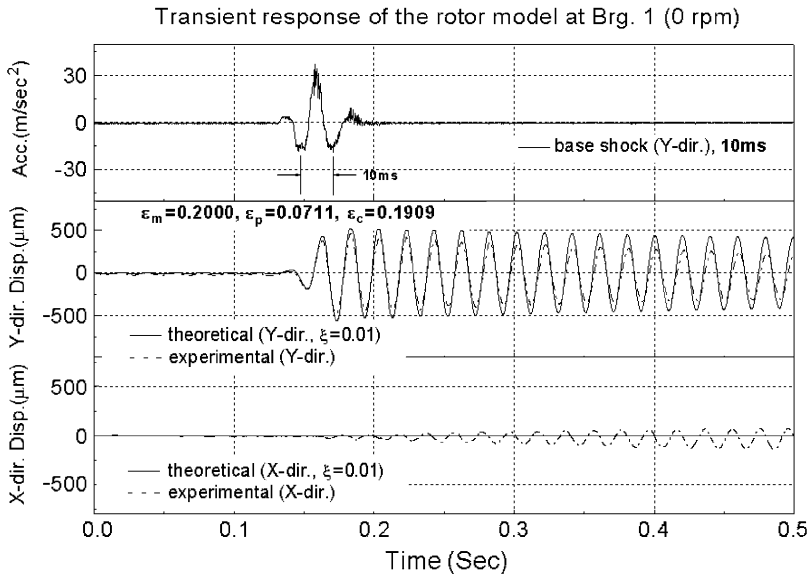

Fig. 12. Experimental shock wave with a duration time of 10 ms and analytical and experimental rotor responses at bearing 1 for 0 rev/min.

4.3. Comparisons of analyses and experiments

For the base-transferred shock excitations applied by the shaker at duration times of 5, 10 and 15 ms, the analytical and experimental transient time-responses of the rotor as obtained at bearings 1 and 2 positions are shown in Figs. 10–15 for the stationary state (0 rev/min) and Figs. 16–21 for the rotating state at 6000 rev/min along with their corresponding magnitude, phase and comprehensive error factors, representing quantitative errors. In the analyses the damping ratios of the bearings were set to $\xi = 0.01$.

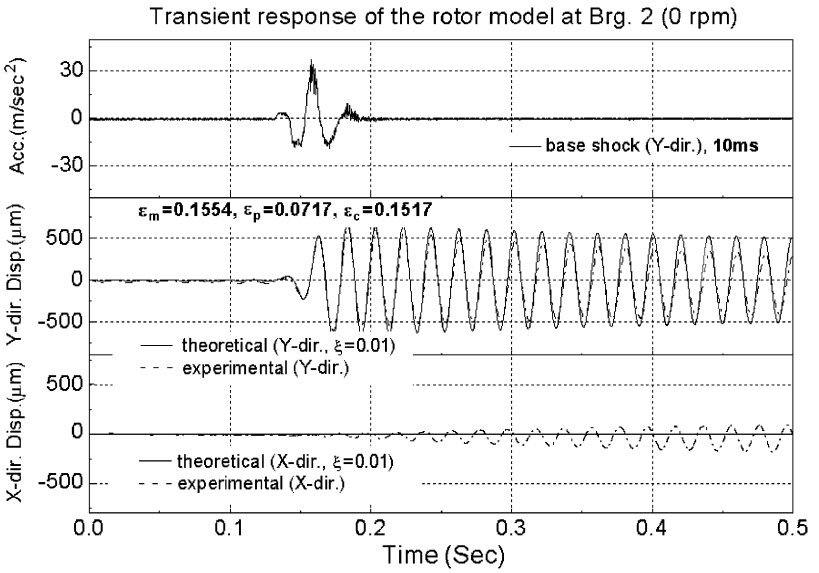

Fig. 13. Experimental shock wave with a duration time of 10 ms and analytical and experimental rotor responses at bearing 2 for 0 rev/min.

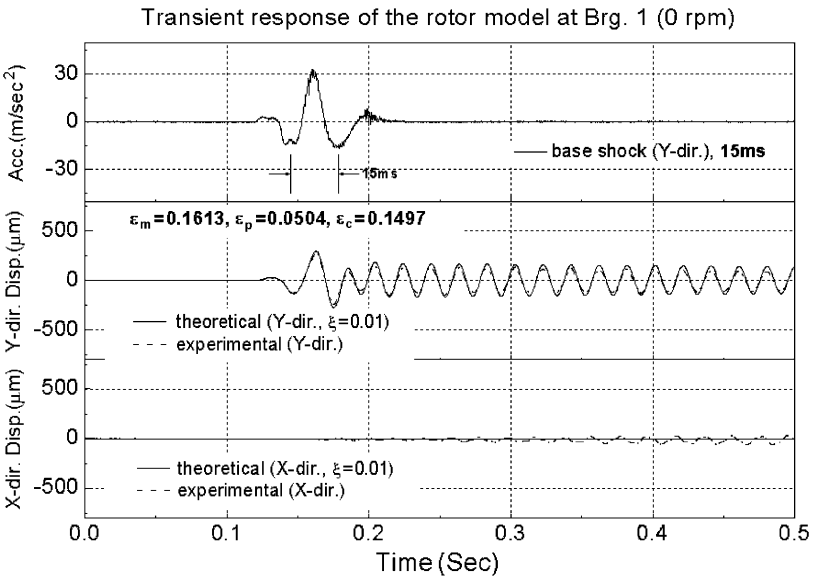

Fig. 14. Experimental shock wave with a duration time of 15 ms and analytical and experimental rotor responses at bearing 1 for 0 rev/min.

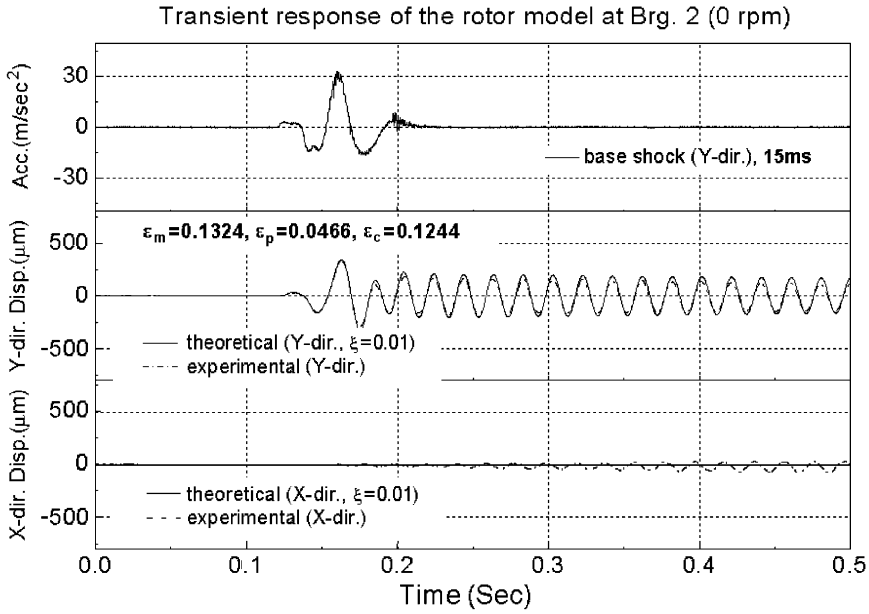

Fig. 15. Experimental shock wave with a duration time of 15 ms and analytical and experimental rotor responses at bearing 2 for 0 rev/min.

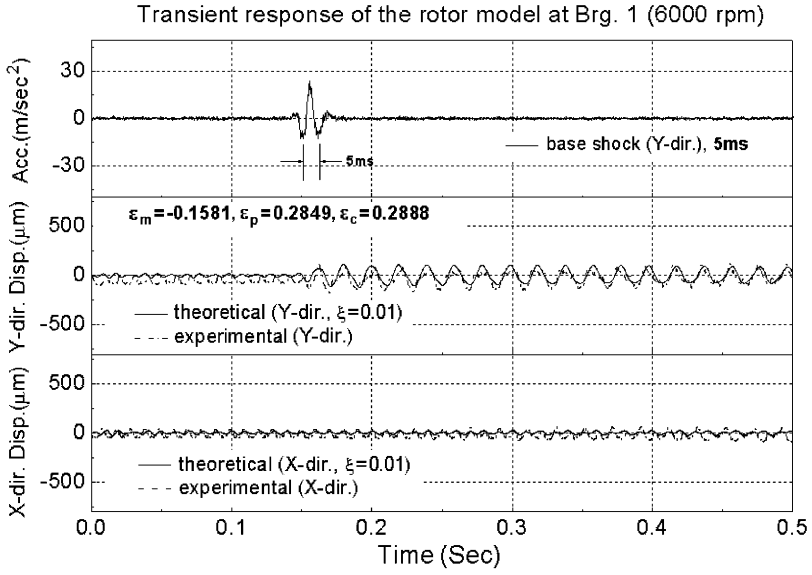

Fig. 16. Experimental shock wave with a duration time of 5 ms and analytical and experimental rotor responses at bearing 1 for 6000 rev/min.

For the stationary state. In the case of duration times of 5, 10 and 15 ms, from Figs. 10–15 the y direction responses of the rotor obtained at bearings 1 and 2 all have ε_m, ε_m and ε_p and ε_c values less than 0.2. Therefore, the analytical and experimental transient time-responses of the rotor to the base-transferred shock excitations were in good agreement with each other. Further, since the shocks were applied only in the y direction and the coupling effects of the bearings were neglected in the analyses, the analytical x direction responses of the rotor were not generated. It was observed that, as in the test rotor the coupling effects

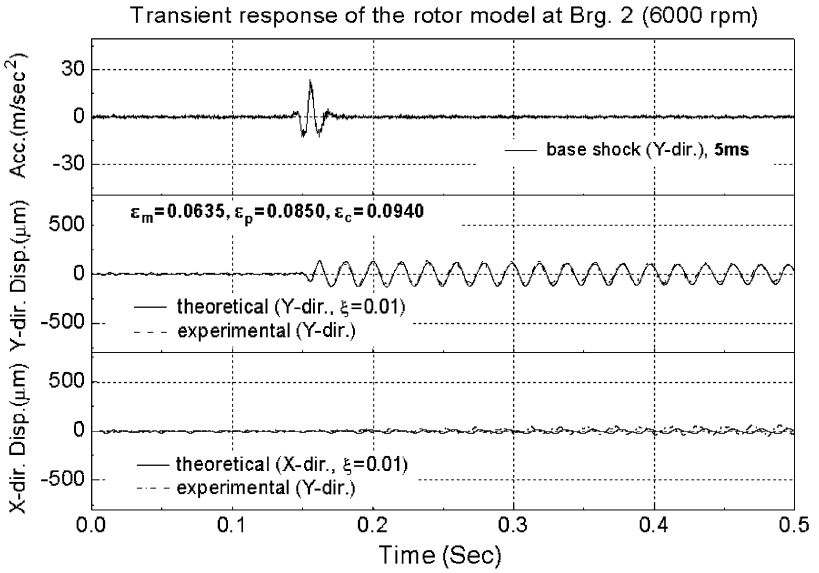

Fig. 17. Experimental shock wave with a duration time of 5 ms and analytical and experimental rotor responses at bearing 2 for 6000 rev/min.

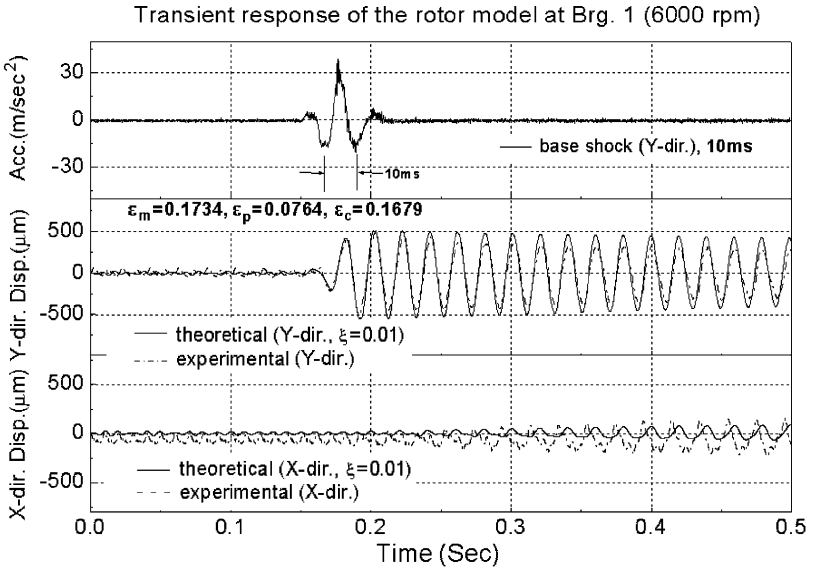

Fig. 18. Experimental shock wave with a duration time of 10 ms and analytical and experimental rotor responses at bearing 1 for 6000 rev/min.

of the bearings acted to some extent, the experimental x direction responses of the rotor increased with increasing time.

For the rotating state. In the case of a duration time of 5 ms, from Fig. 16 the y direction responses of the rotor at bearing 1 have ε_p and ε_c values that are somewhat larger than 0.2 whereas ε_m value is less than 0.2. However, from Fig. 17 the y direction responses of the rotor at bearing 2 all have ε_m, ε_p and ε_c values less than 0.2. In the cases of duration times of 10 and 15 ms, from Figs. 18–21 the y direction responses obtained at bearings 1 and 2 all have ε_m, ε_p and ε_c values less than 0.2. Further, the analytical and experimental x direction responses of the rotor show some differences from each other. Similar to the stationary state, it is reasoned

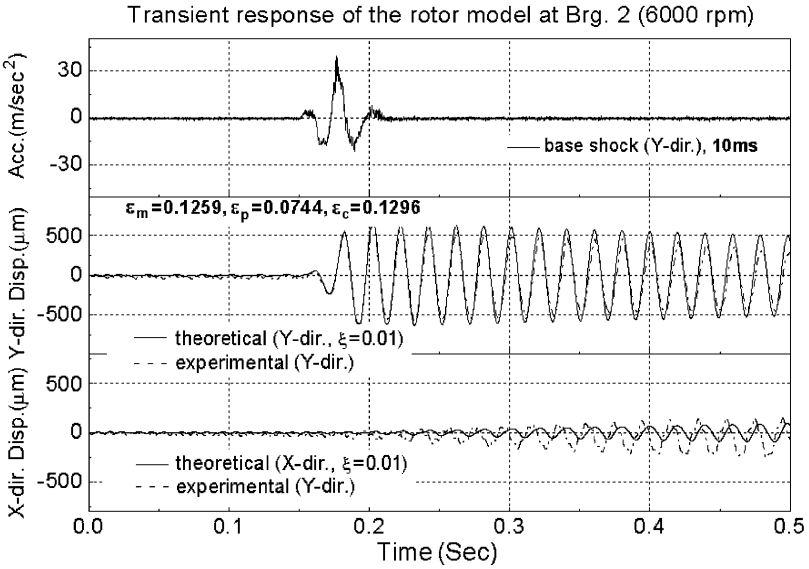

Fig. 19. Experimental shock wave with a duration time of 10 ms and analytical and experimental rotor responses at bearing 2 for 6000 rev/min.

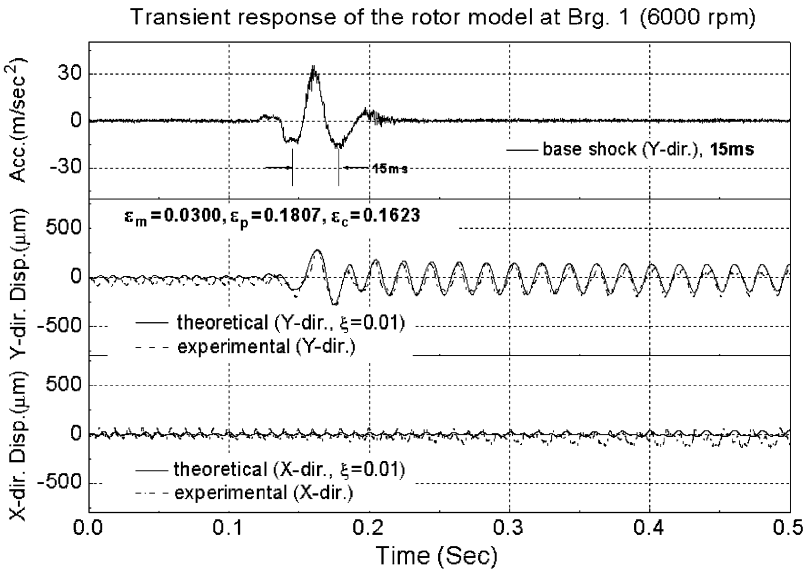

Fig. 20. Experimental shock wave with a duration time of 15 ms and analytical and experimental rotor responses at bearing 1 for 6000 rev/min.

that this is because the analytical model neglected the coupling effects of the bearings whereas in the test rotor the coupling effects of the bearings acted to some extent.

On the other hand, it was observed from Figs. 10–21 that for both 0 and 6000 rev/min the y direction responses of the rotor with a duration time of 10 ms were amplified to a greater extent than those responses with duration times of 5 and 15 ms. The reason for this is that the frequencies, $1/(2 \times \text{duration time}) = 50\,\text{Hz} = 3000\,\text{rev/min}$, of the shock waves with a duration time of 10 ms were close to the natural frequencies or critical speeds (analysis rotor: 3044 rev/min, test rotor: 3060 rev/min) of the rotor-bearing system. From the above, the analytical and experimental transient time-responses of the rotor to the base-transferred shock excitations overall appear to be in good agreement with each other.

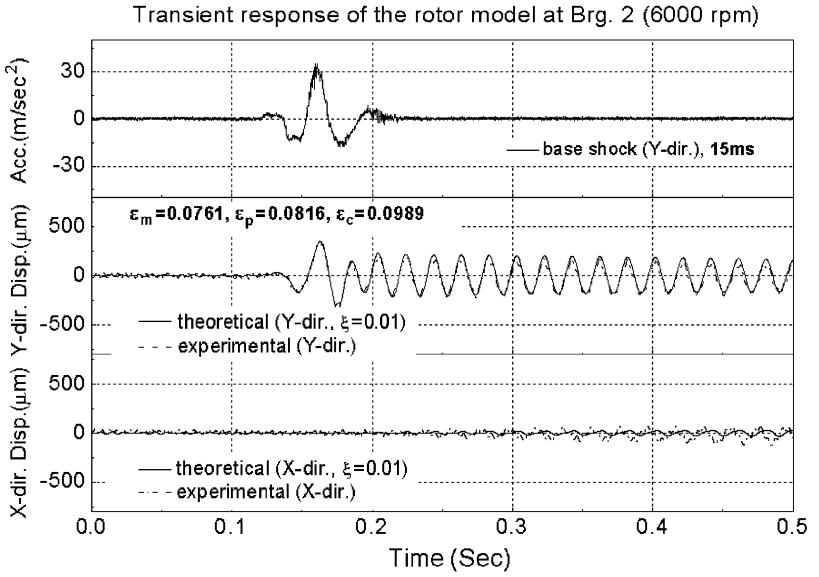

Fig. 21. Experimental shock wave with a duration time of 15 ms and analytical and experimental rotor responses at bearing 2 for 6000 rev/min.

5. Conclusions

In this study a transient response analysis technique of a rotor system was proposed. This technique involved applying the generalized FE modeling method of a rotor-bearing system considering a base-transferred shock force along with the state-space Newmark method of a direct time integration scheme based on the average velocity concept. Experiments were performed to a test rig of a mock-up rotor-bearing system with a series of half-sine shock waves imposed by an electromagnetic shaker, and quantitative error analyses between the analytical and experimental results were carried out. The results showed that the transient responses of the rotor were sensitive to the duration times of the shocks. Particularly, in cases where the frequencies, $1/(2 \times \text{duration time})$, of the shock waves were close to the critical speed of the rotor-bearing system, resonances could occur and the transient responses of the rotor could be amplified. Overall, it is concluded that the analytical results agreed quite well with the experimental data.

Appendix A

A.1. For disk element, system matrices and forcing vectors

$$[M_d] = \begin{bmatrix} m_d & 0 & 0 & 0 \\ 0 & m_d & 0 & 0 \\ 0 & 0 & I_d^t & 0 \\ 0 & 0 & 0 & I_d^t \end{bmatrix}, \tag{A.1}$$

$$[C_d] = \begin{bmatrix} 0 & -2m_d\dot{\theta}_{bZ} & 0 & 0 \\ 2m_d\dot{\theta}_{bZ} & 0 & 0 & 0 \\ 0 & 0 & 0 & -\Omega I_d^p \\ 0 & 0 & \Omega I_d^p & 0 \end{bmatrix}, \tag{A.2}$$

$$[K_d] = \begin{bmatrix} -m_d(\dot{\theta}_{bY}^2 + \dot{\theta}_{bZ}^2) & m_d(\dot{\theta}_{bX}\dot{\theta}_{bY} - \ddot{\theta}_{bZ}) & 0 & 0 \\ -m_d(\dot{\theta}_{bX}\dot{\theta}_{bY} - \ddot{\theta}_{bZ}) & -m_d(\dot{\theta}_{bX}^2 + \dot{\theta}_{bZ}^2) & 0 & 0 \\ 0 & 0 & 0 & 0 \\ 0 & 0 & 0 & 0 \end{bmatrix}, \tag{A.3}$$

$$\{f_{d1}(t)\} = \begin{Bmatrix} -m_d\ddot{u}_{bX} \\ -m_d\ddot{u}_{bY} \\ 0 \\ 0 \end{Bmatrix}, \tag{A.4a}$$

$$\{f_{d2}(t)\} = \begin{Bmatrix} -m_d(\dot{u}_{bZ}\dot{\theta}_{bY} - \dot{u}_{bY}\dot{\theta}_{bZ} + \dot{\theta}_{bX}\dot{\theta}_{bY}h + \dot{\theta}_{bX}\dot{\theta}_{bZ}z) \\ -m_d(\dot{u}_{bX}\dot{\theta}_{bZ} - \dot{u}_{bZ}\dot{\theta}_{bX} - (\dot{\theta}_{bX}^2 + \dot{\theta}_{bZ}^2)h + \dot{\theta}_{bY}\dot{\theta}_{bZ}z) \\ 0 \\ 0 \end{Bmatrix}, \tag{A.4b}$$

$$\{f_{d3}(t)\} = \begin{Bmatrix} -m_d(\ddot{\theta}_{bY}z - \ddot{\theta}_{bZ}h) \\ m_d\ddot{\theta}_{bX}z \\ -(I_d^t\ddot{\theta}_{bX} + I_d^p\Omega\dot{\theta}_{bY}) \\ -(I_d^t\ddot{\theta}_{bY} - I_d^p\Omega\dot{\theta}_{bX}) \end{Bmatrix}. \tag{A.4c}$$

Appendix B. For shaft element, system matrices and forcing vectors

$$[M_s^t] = [M_s^t]_0 + \sigma[M_s^t]_1 + \sigma^2[M_s^t]_2, \quad \sigma = \frac{12EI_s^t}{\kappa GAl^2}, \tag{B.1}$$

where

$$[M_s^t]_0 = \frac{\rho Al}{420(1+\sigma)^2} \begin{bmatrix} 156 & & & & & & & \\ 0 & 156 & & & & \text{SYM} & & \\ 0 & -22l & 4l^2 & & & & & \\ 22l & 0 & 0 & 4l^2 & & & & \\ 54 & 0 & 0 & 13l & 156 & & & \\ 0 & 54 & -13l & 0 & 0 & 156 & & \\ 0 & 13l & -3l^2 & 0 & 0 & 22l & 4l^2 & \\ -13l & 0 & 0 & -3l^2 & -22l & 0 & 0 & 4l^2 \end{bmatrix}, \tag{B.1a}$$

$$[M_s^t]_1 = \frac{\rho Al}{420(1+\sigma)^2} \begin{bmatrix} 294 & & & & & & & \\ 0 & 294 & & & & \text{SYM} & & \\ 0 & -38.5l & 7l^2 & & & & & \\ 38.5l & 0 & 0 & 7l^2 & & & & \\ 126 & 0 & 0 & 31.5l & 294 & & & \\ 0 & 126 & -31.5l & 0 & 0 & 294 & & \\ 0 & 31.5l & -7l^2 & 0 & 0 & 38.5l & 7l^2 & \\ -31.5l & 0 & 0 & -7l^2 & -38.5l & 0 & 0 & 7l^2 \end{bmatrix}, \tag{B.1b}$$

$$[M_s^t]_2 = \frac{\rho A l}{420(1+\sigma)^2}\begin{bmatrix} 140 & & & & & & & \\ 0 & 140 & & & & \text{SYM} & & \\ 0 & -17.5l & 3.5l^2 & & & & & \\ 17.5l & 0 & 0 & 3.5l^2 & & & & \\ 70 & 0 & 0 & 17.5l & 140 & & & \\ 0 & 70 & -17.5l & 0 & 0 & 140 & & \\ 0 & 17.5l & -3.5l^2 & 0 & 0 & 17.5l & 3.5l^2 & \\ -17.5l & 0 & 0 & -3.5l^2 & -17.5l & 0 & 0 & 3.5l^2 \end{bmatrix}, \tag{B.1c}$$

$$[M_s^r] = [M_s^r]_0 + \sigma[M_s^r]_1 + \sigma^2[M_s^r]_2, \tag{B.2}$$

where

$$[M_s^r]_0 = \frac{\rho I_s^t}{30l(1+\sigma)^2}\begin{bmatrix} 36 & & & & & & & \\ 0 & 36 & & & & \text{SYM} & & \\ 0 & -3l & 4l^2 & & & & & \\ 3l & 0 & 0 & 4l^2 & & & & \\ -36 & 0 & 0 & -3l & 36 & & & \\ 0 & -36 & 3l & 0 & 0 & 36 & & \\ 0 & -3l & -l^2 & 0 & 0 & 3l & 4l^2 & \\ 3l & 0 & 0 & -l^2 & -3l & 0 & 0 & 4l^2 \end{bmatrix}, \tag{B.2a}$$

$$[M_s^r]_1 = \frac{\rho I_s^t}{30l(1+\sigma)^2}\begin{bmatrix} 0 & & & & & & & \\ 0 & 0 & & & & \text{SYM} & & \\ 0 & 15l & 5l^2 & & & & & \\ -15l & 0 & 0 & 5l^2 & & & & \\ 0 & 0 & 0 & 15l & 0 & & & \\ 0 & 0 & -15l & 0 & 0 & 0 & & \\ 0 & 15l & -5l^2 & 0 & 0 & -15l & 5l^2 & \\ -15l & 0 & 0 & -5l^2 & 15l & 0 & 0 & 5l^2 \end{bmatrix}, \tag{B.2b}$$

$$[M_s^r]_2 = \frac{\rho I_s^t}{30l(1+\sigma)^2}\begin{bmatrix} 0 & & & & & & & \\ 0 & 0 & & & & \text{SYM} & & \\ 0 & 0 & 10l^2 & & & & & \\ 0 & 0 & 0 & 10l^2 & & & & \\ 0 & 0 & 0 & 0 & 0 & & & \\ 0 & 0 & 0 & 0 & 0 & 0 & & \\ 0 & 0 & 5l^2 & 0 & 0 & 0 & 10l^2 & \\ 0 & 0 & 0 & 5l^2 & 0 & 0 & 0 & 10l^2 \end{bmatrix}, \tag{B.2c}$$

$$[C_s^g] = [C_s^g]_0 + \sigma[C_s^g]_1 + \sigma^2[C_s^g]_2. \tag{B.3}$$

where

$$[C_s^g]_0 = \frac{2\rho I_s^t}{30l(1+\sigma)^2}\begin{bmatrix} 0 & & & & & & & \\ -36 & 0 & & & \text{SKEW} & \text{SYM} & & \\ 3l & 0 & 0 & & & & & \\ 0 & 3l & -4l^2 & 0 & & & & \\ 0 & -36 & 3l & 0 & 0 & & & \\ 36 & 0 & 0 & 3l & -36 & 0 & & \\ 3l & 0 & 0 & -l^2 & -3l & 0 & 0 & \\ 0 & 3l & l^2 & 0 & 0 & -3l & -4l^2 & 0 \end{bmatrix}, \tag{B.3a}$$

$$[C_s^g]_1 = \frac{2\rho I_s^t}{30l(1+\sigma)^2}\begin{bmatrix} 0 & & & & & & & \\ 0 & 0 & & & \text{SKEW} & \text{SYM} & & \\ -15l & 0 & 0 & & & & & \\ 0 & -15l & -5l^2 & 0 & & & & \\ 0 & 0 & -15l & 0 & 0 & & & \\ 0 & 0 & 0 & -15l & 0 & 0 & & \\ -15l & 0 & 0 & -5l^2 & 15l & 0 & 0 & \\ 0 & -15l & 5l^2 & 0 & 0 & 15l & -5l^2 & 0 \end{bmatrix}, \tag{B.3b}$$

$$[C_s^g]_2 = \frac{2\rho I_s^t}{30l(1+\sigma)^2}\begin{bmatrix} 0 & & & & & & & \\ 0 & 0 & & & \text{SKEW} & \text{SYM} & & \\ 0 & 0 & 0 & & & & & \\ 0 & 0 & -10l^2 & 0 & & & & \\ 0 & 0 & 0 & 0 & 0 & & & \\ 0 & 0 & 0 & 0 & 0 & 0 & & \\ 0 & 0 & 0 & 5l^2 & 0 & 0 & 0 & \\ 0 & 0 & -5l^2 & 0 & 0 & 0 & -10l^2 & 0 \end{bmatrix}, \tag{B.3c}$$

$$[C_s^p] = [C_s^p]_0 + \sigma[C_s^p]_1 + \sigma^2[C_s^p]_2, \tag{B.4}$$

where

$$[C_s^p]_0 = \frac{\rho A l}{420(1+\sigma)^2}\begin{bmatrix} 0 & & & & & & & \\ 312 & 0 & & & \text{SKEW} & \text{SYM} & & \\ -44l & 0 & 0 & & & & & \\ 0 & -44l & 8l^2 & 0 & & & & \\ 0 & -108 & 26l & 0 & 0 & & & \\ 108 & 0 & 0 & 26l & 312 & 0 & & \\ 26l & 0 & 0 & 6l^2 & 44l & 0 & 0 & \\ 0 & 26l & -6l^2 & 0 & 0 & 44l & 8l^2 & 0 \end{bmatrix}, \tag{B.4a}$$

$$[C_s^p]_1 = \frac{\rho A l}{420(1+\sigma)^2}\begin{bmatrix} 0 & & & & & & & \\ 588 & 0 & & & \text{SKEW} & \text{SYM} & & \\ -77l & 0 & 0 & & & & & \\ 0 & -77l & 14l^2 & 0 & & & & \\ 0 & -252 & 63l & 0 & 0 & & & \\ 252 & 0 & 0 & 63l & 588 & 0 & & \\ 63l & 0 & 0 & 14l^2 & 77l & 0 & 0 & \\ 0 & 63l & -14l^2 & 0 & 0 & 77l & 14l^2 & 0 \end{bmatrix}, \tag{B.4b}$$

$$[C_s^p]_2 = \frac{\rho A l}{420(1+\sigma)^2}\begin{bmatrix} 0 & & & & & & & \\ 280 & 0 & & & \text{SKEW} & \text{SYM} & & \\ -35l & 0 & 0 & & & & & \\ 0 & -35l & 7l^2 & 0 & & & & \\ 0 & -140 & 35l & 0 & 0 & & & \\ 35 & 0 & 0 & 35l & 280 & 0 & & \\ 35l & 0 & 0 & 7l^2 & 35l & 0 & 0 & \\ 0 & 35l & -7l^2 & 0 & 0 & 35l & 7l^2 & 0 \end{bmatrix}, \tag{B.4c}$$

$$[K_s^e] = [K_s^e]_0 + \sigma[K_s^e]_1, \tag{B.5}$$

where

$$[K_s^e]_0 = \frac{EI_s^t}{l^3(1+\sigma)}\begin{bmatrix} 12 & & & & & & & \\ 0 & 12 & & & & \text{SYM} & & \\ 0 & -6l & 4l^2 & & & & & \\ 6l & 0 & 0 & 4l^2 & & & & \\ -12 & 0 & 0 & -6l & 12 & & & \\ 0 & -12 & 6l & 0 & 0 & 12 & & \\ 0 & -6l & 2l^2 & 0 & 0 & 6l & 4l^2 & \\ 6l & 0 & 0 & 2l^2 & -6l & 0 & 0 & 4l^2 \end{bmatrix}, \tag{B.5a}$$

$$[K_s^e]_1 = \frac{EI_s^t}{l^3(1+\sigma)}\begin{bmatrix} 0 & & & & & & & \\ 0 & 0 & & & & \text{SYM} & & \\ 0 & 0 & l^2 & & & & & \\ 0 & 0 & 0 & l^2 & & & & \\ 0 & 0 & 0 & 0 & 0 & & & \\ 0 & 0 & 0 & 0 & 0 & 0 & & \\ 0 & 0 & -l^2 & 0 & 0 & 0 & l^2 & \\ 0 & 0 & 0 & -l^2 & 0 & 0 & 0 & l^2 \end{bmatrix}, \tag{B.5b}$$

$$[K_s^c] = [K_s^c]_0 + \sigma[K_s^c]_1 + \sigma^2[K_s^c]_2, \tag{B.6}$$

where

$$[K_s^c]_0 = \frac{\rho Al}{840(1+\sigma)^2}\begin{bmatrix} -312\varepsilon_1 & & & & & & & \\ 312\varepsilon_3 & -312\varepsilon_2 & & & & \text{SYM} & & \\ -44l\varepsilon_3 & 44l\varepsilon_2 & -8l^2\varepsilon_2 & & & & & \\ -44l\varepsilon_1 & 44l\varepsilon_3 & -8l^2\varepsilon_3 & -8l^2\varepsilon_1 & & & & \\ -108\varepsilon_1 & 108\varepsilon_3 & -26l\varepsilon_3 & -26l\varepsilon_1 & -312\varepsilon_1 & & & \\ 108\varepsilon_3 & -108\varepsilon_2 & 26l\varepsilon_2 & 26l\varepsilon_3 & 312\varepsilon_3 & -312\varepsilon_2 & & \\ 26l\varepsilon_3 & -26l\varepsilon_2 & 6l^2\varepsilon_2 & 6l^2\varepsilon_3 & 44l\varepsilon_3 & -44l\varepsilon_2 & -8l^2\varepsilon_2 & \\ 26l\varepsilon_1 & -26l\varepsilon_3 & 6l^2\varepsilon_3 & 6l^2\varepsilon_1 & 44l\varepsilon_1 & -44l\varepsilon_3 & -8l^2\varepsilon_3 & -8l^2\varepsilon_1 \end{bmatrix}, \tag{B.6a}$$

$$\varepsilon_1 = (\dot{\theta}_{bY}^2 + \dot{\theta}_{bZ}^2), \quad \varepsilon_2 = (\dot{\theta}_{bX}^2 + \dot{\theta}_{bZ}^2), \quad \varepsilon_3 = \dot{\theta}_{bX}\dot{\theta}_{bY},$$

$$[K_s^c]_1 = \frac{\rho Al}{840(1+\sigma)^2}\begin{bmatrix} -588\varepsilon_1 & & & & & & & \\ 588\varepsilon_3 & -588\varepsilon_2 & & & & \text{SYM} & & \\ -77l\varepsilon_3 & 77l\varepsilon_2 & -14l^2\varepsilon_2 & & & & & \\ -77l\varepsilon_1 & 77l\varepsilon_3 & -14l^2\varepsilon_3 & -14l^2\varepsilon_1 & & & & \\ -252\varepsilon_1 & 252\varepsilon_3 & -63l\varepsilon_3 & -63l\varepsilon_1 & -588\varepsilon_1 & & & \\ 252\varepsilon_3 & -252\varepsilon_2 & 63l\varepsilon_2 & 63l\varepsilon_3 & 588\varepsilon_3 & -588\varepsilon_2 & & \\ 63l\varepsilon_3 & -63l\varepsilon_2 & 14l^2\varepsilon_2 & 14l^2\varepsilon_3 & 77l\varepsilon_3 & -77l\varepsilon_2 & -14l^2\varepsilon_2 & \\ 63l\varepsilon_1 & -63l\varepsilon_3 & 14l^2\varepsilon_3 & 14l^2\varepsilon_1 & 77l\varepsilon_1 & -77l\varepsilon_3 & -14l^2\varepsilon_3 & -14l^2\varepsilon_1 \end{bmatrix}, \tag{B.6b}$$

$$[K_s^c]_2 = \frac{\rho Al}{840(1+\sigma)^2}\begin{bmatrix} -280\varepsilon_1 & & & & & & & \\ 280\varepsilon_3 & -280\varepsilon_2 & & & & \text{SYM} & & \\ -35l\varepsilon_3 & 35l\varepsilon_2 & -7l^2\varepsilon_2 & & & & & \\ -35l\varepsilon_1 & 35l\varepsilon_3 & -7l^2\varepsilon_3 & -7l^2\varepsilon_1 & & & & \\ -140\varepsilon_1 & 140\varepsilon_3 & -35l\varepsilon_3 & -35l\varepsilon_1 & -280\varepsilon_1 & & & \\ 140\varepsilon_3 & -140\varepsilon_2 & 35l\varepsilon_2 & 35l\varepsilon_3 & 280\varepsilon_3 & -280\varepsilon_2 & & \\ 35l\varepsilon_3 & -35l\varepsilon_2 & 7l^2\varepsilon_2 & 7l^2\varepsilon_3 & 35l\varepsilon_3 & -35l\varepsilon_2 & -7l^2\varepsilon_2 & \\ 35l\varepsilon_1 & -35l\varepsilon_3 & 7l^2\varepsilon_3 & 7l^2\varepsilon_1 & 35l\varepsilon_1 & -35l\varepsilon_3 & -7l^2\varepsilon_3 & -7l^2\varepsilon_1 \end{bmatrix}, \tag{B.6c}$$

$$[K_s^a] = [K_s^a]_0 + \sigma[K_s^a]_1 + \sigma^2[K_s^a]_2, \tag{B.7}$$

where

$$[K_s^a]_0 = \frac{1}{2}[C_s^p]_0, \quad [K_s^a]_1 = \frac{1}{2}[C_s^p]_1, \quad [K_s^a]_2 = \frac{1}{2}[C_s^p]_2, \tag{B.7a}$$

$$\{f_{s1}(t)\} = \frac{\rho Al}{12}\begin{Bmatrix} -6\ddot{u}_{bX} \\ -6\ddot{u}_{bY} \\ l\ddot{u}_{bY} \\ -l\ddot{u}_{bX} \\ -6\ddot{u}_{bX} \\ -6\ddot{u}_{bY} \\ -l\ddot{u}_{bY} \\ l\ddot{u}_{bX} \end{Bmatrix}, \tag{B.8a}$$

$$\{f_{s2}(t)\} = \frac{\rho Al}{12}\begin{Bmatrix} -6(\dot{\theta}_{bX}\dot{\theta}_{bY}h - \dot{\theta}_{bZ}\dot{u}_{bY} + \dot{\theta}_{bY}\dot{u}_{bZ} + \dot{\theta}_{bX}\dot{\theta}_{bZ}z) \\ 6(\dot{\theta}_{bX}^2 h + \dot{\theta}_{bX}\dot{u}_{bZ} + \dot{\theta}_{bZ}^2 h - \dot{\theta}_{bZ}\dot{u}_{bX} - \dot{\theta}_{bZ}\dot{\theta}_{bY}z) \\ -l(\dot{\theta}_{bX}^2 h + \dot{\theta}_{bX}\dot{u}_{bZ} + \dot{\theta}_{bZ}^2 h - \dot{\theta}_{bZ}\dot{u}_{bX} - \dot{\theta}_{bZ}\dot{\theta}_{bY}z) \\ -l(\dot{\theta}_{bX}\dot{\theta}_{bY}h - \dot{\theta}_{bZ}\dot{u}_{bY} + \dot{\theta}_{bY}\dot{u}_{bZ} + \dot{\theta}_{bX}\dot{\theta}_{bZ}z) \\ -6(\dot{\theta}_{bX}\dot{\theta}_{bY}h - \dot{\theta}_{bZ}\dot{u}_{bY} + \dot{\theta}_{bY}\dot{u}_{bZ} + \dot{\theta}_{bX}\dot{\theta}_{bZ}z) \\ 6(\dot{\theta}_{bX}^2 h + \dot{\theta}_{bX}\dot{u}_{bZ} + \dot{\theta}_{bZ}^2 h - \dot{\theta}_{bZ}\dot{u}_{bX} - \dot{\theta}_{bZ}\dot{\theta}_{bY}z) \\ l(\dot{\theta}_{bX}^2 h + \dot{\theta}_{bX}\dot{u}_{bZ} + \dot{\theta}_{bZ}^2 h - \dot{\theta}_{bZ}\dot{u}_{bX} - \dot{\theta}_{bZ}\dot{\theta}_{bY}z) \\ l(\dot{\theta}_{bX}\dot{\theta}_{bY}h - \dot{\theta}_{bZ}\dot{u}_{bY} + \dot{\theta}_{bY}\dot{u}_{bZ} + \dot{\theta}_{bX}\dot{\theta}_{bZ}z) \end{Bmatrix}, \tag{B.8b}$$

$$\{f_{s3}(t)\} = \frac{\rho Al}{12}\begin{Bmatrix} -6(\ddot{\theta}_{bZ}h - \ddot{\theta}_{bY}z) \\ 6\ddot{\theta}_{bX}z \\ -l\ddot{\theta}_{bX}z \\ l(\ddot{\theta}_{bZ}h - \ddot{\theta}_{bY}z) \\ 6(\ddot{\theta}_{bZ}h - \ddot{\theta}_{bY}z) \\ 6\ddot{\theta}_{bX}z \\ l\ddot{\theta}_{bX}z \\ -l(\ddot{\theta}_{bZ}h - \ddot{\theta}_{bY}z) \end{Bmatrix} + \frac{\Omega\rho I_s^t}{1+\sigma}\begin{Bmatrix} 2\dot{\theta}_{bX} \\ 2\dot{\theta}_{bY} \\ l\dot{\theta}_{bY} \\ -l\dot{\theta}_{bX} \\ -2\dot{\theta}_{bX} \\ -2\dot{\theta}_{bY} \\ l\dot{\theta}_{bY} \\ -l\dot{\theta}_{bX} \end{Bmatrix} + \frac{\rho I_s^t}{2(1+\sigma)}\begin{Bmatrix} 2\ddot{\theta}_{bX} \\ -2\ddot{\theta}_{bY} \\ -\sigma l\ddot{\theta}_{bX} \\ -\sigma l\ddot{\theta}_{bY} \\ -2\ddot{\theta}_{bY} \\ 2\ddot{\theta}_{bX} \\ -\sigma l\ddot{\theta}_{bX} \\ -\sigma l\ddot{\theta}_{bY} \end{Bmatrix}. \tag{B.8c}$$

References

[1] Y. Hori, T. Kato, Earthquake-induced instability of a rotor supported by oil film bearings, *ASME Journal of Vibration and Acoustics* 112 (1992) 160–165.

[2] J.M. Tessarzik, T. Chiang, R.H. Badgley, The response of rotating machinery to external random vibration, *ASME Journal of Engineering for Industry* 96 (1974) 477–489.

[3] A.H. Soni, V. Srinivasan, Seismic analysis of a gyroscopic mechanical system, *ASME Journal of Vibration, Acoustics, Stress, and Reliability in Design* 105 (1983) 449–455.

[4] M.P. Singh, T.S. Chang, L.E. Suarez, A response spectrum method for seismic design evaluation of rotating machines, *ASME Journal of Vibration and Acoustics* 114 (1992) 454–460.

[5] L.E. Suarez, M.P. Singh, M.S. Rohanimanesh, Seismic response of rotating machines, *Earthquake Engineering and Structural Dynamics* 21 (1992) 21–36.

[6] B.J. Gaganis, A.K. Zisimopoulos, P.G. Nikolakopoulos, C.A. Papadopoulos, Modal analysis of rotor on piecewise linear journal bearings under seismic excitation, *ASME Journal of Vibration and Acoustics* 121 (1999) 190–196.

[7] T.J.R. Hughes, *The Finite Element Method: Linear Static and Dynamic Finite Element Analysis*, First ed, Prentice-Hall, Englewood Cliffs, NJ, 1987.

[8] J.L. Humar, *Dynamics of Structures*, First ed., Prentice-Hall, Englewood Cliffs, NJ, 1990.

[9] B.O. Kim, A.S. Lee, A transient response analysis in the state-space applying the average velocity concept, *Journal of Sound and Vibration* 281 (2005) 1023–1035.

[10] H.D. Nelson, A finite rotating shaft element using timoshenko beam theory, *ASME Journal of Mechanical Design* 102 (1980) 793–803.

[11] D.M. Russell, Error measures for comparing transient data: part I: development of a comprehensive error measure, *Electric Boat Corporation* (1995) 175–184.